



# Application of Bioactive Nano-Glass Fiber in Combination with Fresh Platelet-Rich Plasma on the Re-Epithelialization of the Thermal Wound in Rats

Reza Esmaealzade Dizaji<sup>1</sup>, Arasb Dabbagh Moghaddam<sup>1\*</sup>, Arash Ghalyanchi Langeroudi<sup>2</sup>, Mohamad Foad Heydari<sup>3</sup>, Seyyed Javad Hosseini Shokouh<sup>4</sup> and Ana Shirzad Shahrivar<sup>5</sup>

<sup>1</sup>Department of Health, School of Health, Science and Research Branch, AJA University of Medical Sciences, Tehran, Iran

<sup>2</sup>Department of Microbiology and Immunology, Faculty of Veterinary Medicine, University of Tehran, Tehran, Iran

<sup>3</sup>Department of Medical Laboratory Sciences, School of Allied Health Medicine, AJA University of Medical Sciences, Tehran, Iran

<sup>4</sup>Department of Infectious Disease Research Center, Faculty of Medicine, AJA University of Medical Sciences, Tehran, Iran

<sup>5</sup>Department of Nursing, Faculty of Medical science, University of Azad Islamic Ardabil Branch, Iran

## ABSTRACT

In this study, topical application of bioactive nano-glass fibers (BNF) loaded with platelet-rich plasma (PRP) was used to examine the effects on a second-degree heat wound and the healing process' sub-streaming molecular route for re-epithelialization. Model (deep second-degree thermal wound), PRP, and PRP/BNF groups were each randomly assigned a set of animals. Wounds were monitored daily for many days following therapy to see how they were healing. H&E staining and qRT-PCR were used to examine the pathological alterations in wound tissues and to determine mRNA expression of inflammatory and pro-inflammatory cytokines. We found that the PRP/BNF group and the PRP group had faster wound healing rates than the model group at each time point in the current investigation. The same results were corroborated by the pathological score of skin wounds stained with H&E. Researchers found that in comparison to the control group, those in both the PRP/BNF and PRP groups had significantly lower expression levels of the mRNAs for interleukin 1, interleukin 6, and interleukin 10 than those in the untreated group. In contrast, those in the untreated group had significantly higher expression levels of those genes. The PRP/BNF and PRP promote wound epithelization by raising the expression of EGF, VEGF, TGF- $\beta$ , HIF-1, and Integrin 3, while boosting the release of Integrin 1 and other mechanisms, reducing healing time and improving healing quality.

## Article Information

Received 01 December 2021

Revised 05 June 2022

Accepted 13 July 2022

Available online 03 August 2022

(early access)

Published 28 August 2023

## Authors' Contribution

RED presented the concept, supplied raw materials and wrote the manuscript. ADM and AGL supervised the study. MFH, ADM and AGL edited the manuscript. RED and MFH analysis data. SJHS helped in the analysis. ASS and RED performed the experiments. ASS helped to write the manuscript.

## Key words

Deep second-degree thermal wound, Wound healing, Re-epithelialization, Fresh Platelet rich plasma, Bioactive nano-glass fiber

## INTRODUCTION

The most prevalent type of skin injury is related to burn injuries. Epidermal stem cells (ESCs) and sebaceous

gland stem cells (SGs) can help cure second-degree burns and the deep dermis layer. Chronic necrosis and subsequent infections can lead to an overly inflammatory response at the site of the wound, prolonging healing time or causing hyperplastic scarring, which has a negative impact on how well a wound heals. As a result, scar-free healing can be achieved if the deep second-degree scald lesion is treated appropriately. Re-epithelialization and repair of ESCs in the skin tissue are involved in this process. Researchers discovered that ESCs are present in the basal cells of the epidermis as well as in hair follicles, sebaceous glands, and other skin appendages (Morasso and Tomic-Canic, 2005; Sun et al., 2013; Peacock et al., 2015). These ESCs not only aid in the regeneration of the epidermis, but

\* Corresponding author: [arasbdabbaghmoghadam@gmail.com](mailto:arasbdabbaghmoghadam@gmail.com)  
0030-9923/2023/0005-2265 \$ 9.00/0



Copyright 2023 by the authors. Licensee Zoological Society of Pakistan.

This article is an open access article distributed under the terms and conditions of the Creative Commons Attribution (CC BY) license (<https://creativecommons.org/licenses/by/4.0/>).

they also aid in the repair of injuries (Choi *et al.*, 2015). It is now well accepted that re-epithelialization, or re-epithelialization, is a critical part of burns treatment and has become an important research area both domestically and internationally. The re-epithelialization of skin wound healing involves numerous key links: the migration and proliferation of epidermal cells, the reorganization of collagen fibers, and the restoration of skin attachment (Afsar *et al.*, 2017).

The re-epithelialization process relies heavily on EGF, one of the primary growth factors (Levy *et al.*, 2007). EGF has been shown to aid in the healing of wounds, according to studies. Plasma with a high concentration of platelets (Raghavan *et al.*, 2000), known as platelet-rich plasma (PRP), is an autologous product generated from human blood. Centrifugation separates it from the rest of the blood. There are numerous growth factors and cytokines released by activated platelets in PRP, including platelet-derived growth factor (PDGF) and vascular endothelial growth factor (VEF) as well as insulin like growth factor-1 (IGF-1). These growth factors are involved in tissue regeneration, and PRP has been shown to be effective in promoting tissue repair and regeneration (Levy *et al.*, 2007). PRP has been widely used in a variety of surgical procedures and therapeutic therapies because of its ease of preparation, high growth factor content, and low immunogenicity (Tumbar *et al.*, 2004; Levy *et al.*, 2007; Blanpain and Fuchs, 2009).

The development of wound granulation tissue and the re-epithelialization of wounds can also benefit from the use of bioactive glass fiber dressings. PRP also won't adhere to the wound, preventing subsequent injury and alleviating patient discomfort and anxiety associated with changing dressings, both of which have attracted a great deal of attention in the field of biomedical engineering (Takeo *et al.*, 2015).

Current studies have shown that bioactive glass fiber (Harrison *et al.*, 2006; Cao *et al.*, 2014) and sodium carboxymethyl cellulose PRP (Iwamoto *et al.*, 1999; Janes *et al.*, 2002) can promote wound healing, and the skin quality after wound healing is good (Cao *et al.*, 2014). Bioactive nano-glass fibers containing calcium ions and sodium alginate have been proven to stimulate wound re-epithelialization in current research (Iwamoto *et al.*, 1999; Kenny and Connelly, 2015). To understand how bioactive glass fiber works, consider that it might produce a wet environment that encourages the movement of epithelial cells (Levy *et al.*, 2007; Blanpain and Fuchs, 2009). PRP and the novel nano-bioactive glass fiber employed in this study have not yet been proven to stimulate burn wound re-epithelialization, and further research is needed to determine this.

Consequently, the current research seeks to analyze the influence of topically applied bioactive glass fibers loaded PRP on a second-degree heat wound healing process and a molecular route of re-epithelialization sub-stream. The findings of this study may help guide future research into the mechanism of action and potential therapeutic uses.

## MATERIALS AND METHODS

### *Wound healing in an animal model*

Healthy Wistar male rats aged 3-4 months, weighing 200-230 g, SPF grade, were provided by the Medical Laboratory Animal Center of the AJA Medical University. The experimental animals and animal experiment operating procedures used in this study comply with the regulations of the laboratory animal management regulations of the ethics committee of our center, and strictly abide by the 3R principle.

### *Development and testing of a model of second-degree deep scalding in rats*

Rats were anesthetized by intraperitoneal injection of 10% Ketamine (80 mg/kg) + 2% Xylazine (10 mg/kg) after adaptive feeding for 7 days. The dorsal side was shaved with an electric razor, and the center side of the dorsal spine was opened 2 cm left and right as the modeling area. To achieve a second-degree scald burn; a 50 ml plastic centrifuge tube was used which is covered with a single layer of rubber gloves and tied tightly in its mouth (diameter 2.5 cm). It was filled with water to a constant height. The tube was placed upside down in an electric kettle filled with water and retained by pressing to the bottom of the centrifuge tube. The small holes were provided to exhaust. After the electric kettle was energized the water temperature was heated to 95°C, the mouth of the centrifuge tube filled with hot water was placed vertically on the skin of the rat's operation area for 8 s. Local skin whitening and edema were seen, which was an indicator of deep second-degree severe burns. The reliability of the modeling method was verified by pathological sections.

### *Using PRP to treat profound second-degree scalds on rats skin: Delivery technique and experimental grouping*

From total of 80 rats, 20 rats were randomly selected as the normal group, and the remaining 60 rats were randomly divided into 3 groups after modeling: Control group (n=20), PRP group (n=20) and PRP/BNF group (n=20). The normal group received no treatment after routine feeding, the control group was not treated after modeling, the debridement group was locally applied with PRP after the model was built, and the PRP/BNF group

was locally applied with the PRP/BNF after the model was built. The medicine was taken half an hour after making the model. The treatments were applied to cover the wound with a thickness of about 0.5~1.0 mm. The dressings were changed once a day, and the wounds were covered with sterile gauze and then fixed and bandaged to prevent the medicine from falling off. Normal saline (NaCl 0.9 %) was used before each dressing change. Saltwater was used for cleaning the wound and surrounding skin, while no disinfectants were used. After washing, the wound was wiped with a dry cotton swab and the dressing was applied directly. The dressings were changed every day until the 3<sup>rd</sup>, 7<sup>th</sup>, 14<sup>th</sup>, and 21<sup>st</sup> days after the model was created. Applying the therapeutic material to modeled animals was carried out immediately at different time points.

After the rats were modeled, the swelling, color, secretion, scab of the burned area, the time of complete scab removal, and the growth of granulation tissue after scab removal were observed daily. After modeling, a digital camera was provided to take pictures of the wound every three days (n=5) until d 21. When taking images, a scale was placed on the edge of the wound and also, a mirror was kept parallel to the wound. The lens was placed about 11 cm away from the wound. Then the images were saved for evaluation in the future. Image-Pro Plus 6.0 image analysis software was used to measure the wound area with the following formula

$$\text{wound healing rate} = (\text{initial scald wound area} - \text{wound area measured at each time point}) \div \text{initial scald wound area} \times 100.$$

#### *Preparation of bioactive nano-glass fiber*

Deionized water was obtained from a water purification system (Millipore SAS, France). The 45S5 bioactive glass (45S5) (weight compositions: 45% SiO<sub>2</sub>, 24.5% Na<sub>2</sub>O, 24.5% CaO, and 6% P<sub>2</sub>O<sub>5</sub>) was prepared by a melting process in this study by mixing the analytical reagent grades Na<sub>2</sub>CO<sub>3</sub>, CaCO<sub>3</sub>, Na<sub>3</sub>PO<sub>4</sub>, and SiO<sub>2</sub> in an electric oven at 1400 °C for 2h (Truong et al., 2006). The 58S sol-gel bioactive glass (SGBG-58S) (weight composition: 58% SiO<sub>2</sub>, 33% CaO, and 9% P<sub>2</sub>O<sub>5</sub>) was prepared by the sol-gel method. Briefly, the sol was made by hydrolysis of TEOS, TEP, and Ca (NO<sub>3</sub>)<sub>2</sub>·4H<sub>2</sub>O. After ageing the sol at 70 °C for three days followed by drying at 150 °C for two days, the gel was obtained. Later, the gel was heated for 2 h at 700 °C to get sol-gel 58S bioglass (Blanpain and Fuchs, 2009). The synthesis procedure for the nano bioactive glass (NBG-58S) (weight composition: 58% SiO<sub>2</sub>, 33% CaO, and 9% P<sub>2</sub>O<sub>5</sub>) was as follows (Levy et al., 2007): TEOS (221.02 mL) and CN (138.68 g) were mixed with EA (162.21 mL, ethanol: deionized water = 1:1) to form a solution, using HCl to adjust the pH between 1

and 2 to form a sol. A DAP solution containing DAP (17.4 g) and deionized water was also prepared. Then the TEOS-CN-EA solution was slowly added to the DAP solution while stirring. Once the two solutions were completely mixed, a solution of ammonia (28%wt, a gelation catalyst) was added dropwise to the mixture until a white precipitate appeared. Finally, the bioactive glass was obtained after freeze-drying the sol-gel co-precipitate and heating at 600°C.

All types of bioactive glasses were fabricated into particles with diameters less than 53 µm by grinding and sieving using a sieve shaker (Vibratory Sieve Shaker AS 200 control, Germany). The morphology of the bioactive glasses was observed using a scanning electron microscope (SEM, Tecnai 12, FEI, The Netherlands) under an accelerating voltage of 10.0 kV.

The bioactive glass solutions were then prepared by the following method: bioactive glass powders (18 wt%) were mixed with melted Vaseline (maintained at 80 °C) under vigorous stirring, then cooled and sterilized.

#### *Preparation platelet rich plasma (PRP)*

The rats were anesthetized with intraperitoneal injection of 10% Ketamine (80 mg/kg) + 2% Xylazine (10 mg/kg). PRP was obtained through centrifugation of inferior vena cava blood collected from healthy mice into 0.3% heparin sodium anticoagulant tubes. The plasma was first collected by centrifugation (300 × g, 10 min). Platelets in the plasma were then concentrated through second centrifugation (300 × g, 20 min). Approximately 10 mL of whole blood can produce an average of 2–3 mL of PRP, which was activated by the repeated freeze-thaw method.

#### *Histopathological scoring and staining using H & E*

At 4 time points on the 7<sup>th</sup>, 14<sup>th</sup>, and 21<sup>st</sup> days after the scald, 5 rats in each group were immediately selected for cervical dislocation and sacrificed. The skin of the scalded part was cut, fixed in 4% formaldehyde solution, and embedded in paraffin. Sections (3µm thickness) were cut and stained in HE staining. The tissue structure changes of the epidermis and dermis in the wounds of each group were observed under a low-power microscope. The epidermal regeneration, granulocyte infiltration count, new capillary blood vessels, fibroblasts, and collagen under a high-power microscope were observed to score the histopathology of skin wound repair. The histopathological evaluation criteria were carried out according to the methods reported by Eldad et al. (1998) and Zhu et al. (2019).

#### *qRT-PCR detection of mRNA inflammatory and pro-inflammatory cytokines*

Skin wound tissue samples were collected (n=5) at 3,

7, 14, 21 days after scalding from each group, and total RNA was extracted from the samples by the Trizol method (Rio *et al.*, 2010). After reverse transcription to obtain cDNA, the mRNA expression of *KGF*, *TGF- $\beta$* , *IL-1*, *IL-6*, *IL-10*, *EGF*, *VEGF*, *HIF-1 $\alpha$* , *integrin  $\beta$ 1*, and *integrin  $\alpha$ 3* genes were detected and analyzed by fluorescence quantitative PCR. The design and synthesis of PCR primers for the above factors and integrin molecules were completed by AJA University of Medical Sciences (Table I).

**Table I. Listing of primer sequences.**

Genes	Primer sequences (5' → 3')	Product size (bp)
<i>GAPDH</i>	F: GACATGCCGCCTGGAGAAAC R: AGCCCAGGATGCCCTTTAGT	92
<i>KGF</i>	F: GACATGAGTCCAGAGCAGACG R: GGTGCGACAGAACAGTCTCC	120
<i>TGF-<math>\beta</math></i>	F: AATTCCTGGCGTTACCTTGG R: TCTCCTTGGTTCAGCCACTG	107
<i>IL-1</i>	F: TCACAGCAGCATCTCGACAA R: GGTCCTCATCCTGGAAGCTC	112
<i>IL-6</i>	F: TTCCAGCCAGTTGCCTTCTT R: AAGCCTCCGACTTGTGAAGTG	137
<i>IL-10</i>	F: GCAGTGGAGCAGGTGAAGAA R: TCACGTAGGCTTCTATGCAGTTG	106
<i>EGF</i>	F: ACGTTGATGAGTGCCAGCAG R: AAGGCAGTCCAGGTGCTGAT	117
<i>VEGF</i>	F: AGCCTTGTTTCAGAGCGGAGA R: CCTTGGCTTGTCACATCTGC	140
<i>HIF-1<math>\alpha</math></i>	F: CAAGTCAGCAACGTGGAAGG R: ATCAGCACCAAGCACGTCAT	117
<i>Integrin <math>\beta</math>1</i>	F: GTGAACAGCAACGGTGAAGC R: AGCAAGGCAAGGCCAATAAG	125
<i>Integrin <math>\alpha</math>3</i>	F: AGGTGTCATCCGCTCTGCTT R: CAGTCCATCCTCTGGTTC	119

The TaKaRa PrimeScript® RT Reagent Kit (No. RR037A) was used to perform a reverse transcription reaction on total RNA to obtain cDNA. After the system was prepared in the following plan, reverse transcription was performed on a PCR reverse transcription machine. The reaction plan was 37°C for 15 min, 85°C for 5 s. The cDNA samples obtained after reverse transcription were stored in a refrigerator at -20°C.

#### Statistical analysis

All data were statistically analyzed using the SPSS24.0 software package. Histopathological scores were statistically analyzed by rank sum test. Measurement data were expressed as mean  $\pm$  standard deviation (Mean  $\pm$  SD). Analysis of variance was used for sex comparison,

and  $P < 0.05$  indicated that the difference was statistically significant.

## RESULTS

#### Rat skin-deep second-degree scald model

After the preparation of the scald model of rats, the local skin immediately turned pale, slightly swollen, and was separated from the surrounding area, without exudation, and skin elasticity decreased (Fig. 1A). The histological changes (Fig. 1B) indicate that the deep second-degree scald model obtained by the method used in this experiment was successfully modeled.

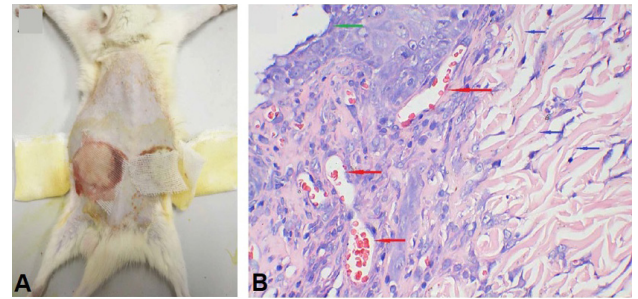


Fig. 1. Preparation of deep second-degree scald model and sti pathological evaluation in rat. A: Skin appearance after scald; B: Histopathological properties of skin after scald by H & E staining ( $\times 100$ ).

#### Deep second degree scald wound in rats

The wound was wet and non-exudative, showing flaky blood stasis and edema. It remained swollen, but no exudation or suppuration had occurred after two days. Three days later, the wound had become brownish-red and shrunk. After four to five days of healing, in the control group, soft scabs developed and cemented on the wounds. The wound edge had a crimson circle around it, but it was not bloated. A red circle appeared around the wound margin in the PRP group after 2 to 3 days, and the soft scabs hardened after 5 to 7 days. After scab removal, some new epithelium was seen around each wound, with granulation tissue in the middle, which is easy to bleed. The complete descaching time of each group is shown in Figure 2; the complete descaching time of the PRP/BNF group ( $11.12 \pm 1.44$  days) is faster than that of the PRP gel group ( $12.33 \pm 1.83$  days) and the control group ( $13.61 \pm 1.62$  days). There was a minor quantity of pale-yellow exudate on the wound, which was at a higher level than normal skin. There was a tiny amount of granulation tissue development in the middle of the wound without exudate on the 21<sup>st</sup> day in the control group. The wound had not yet reached full re-epithelialization. On the 21<sup>st</sup>

day, both the PRP/BNF and the PRP groups had achieved re-epithelialization.

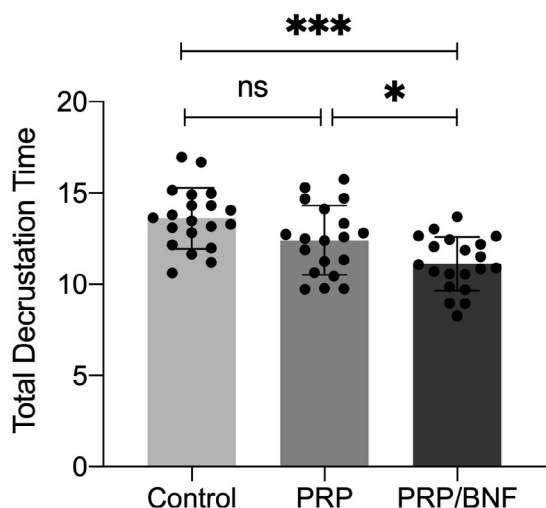


Fig. 2. Total decrustation time of the PRP/BNF therapy for deep second-degree scald in rats (n=20, \*P<0.05, \*\*\*P<0.001, ns: no significance).

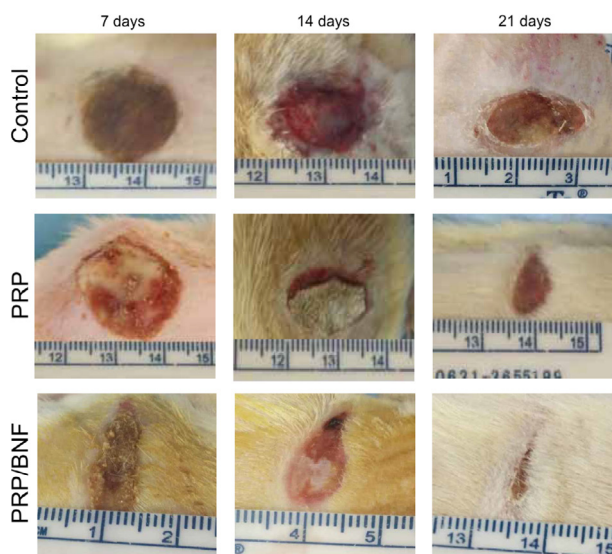


Fig. 3. A general observation of healing process of deep second-degree scald wounds with a PRP/BNF and PRP therapy in comparison to control groups in rats.

*The healing rate of deep second-degree scald wounds in rats*

Using a simple magnifying glass, Figure 3 shows the progression of the scald wounds in each group over time, while Figure 4 shows the wound healing rate data at each of those same time points. Scald injury wound healing

rates were considerably greater in those who received PRP and BNF compared to those who received the control group (P<0.05) on the 3<sup>rd</sup>, 6<sup>th</sup>, 9<sup>th</sup>, 12<sup>th</sup>, 15<sup>th</sup>, 18<sup>th</sup>, and 21<sup>st</sup> days following the injury (P<0.05). Deep second-degree scalds in rats may heal faster with PRP therapy or PRP/BNF treatment, but there is no statistically significant difference in wound healing rates between the PRP group and the PRP/BNF group at any time point (P>0.05).

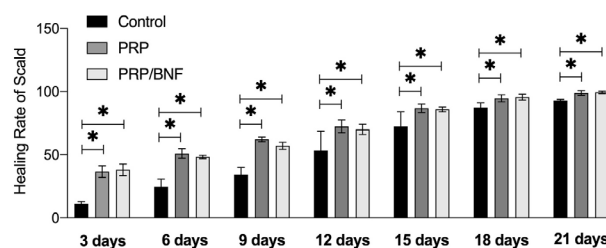


Fig. 4. Changes of wound healing rate in rats treated with PRP/BNF for deep second-degree scald (n=5, \*P<0.05).

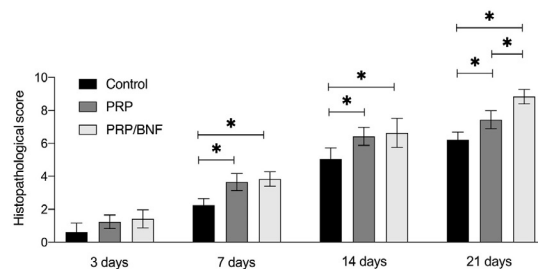
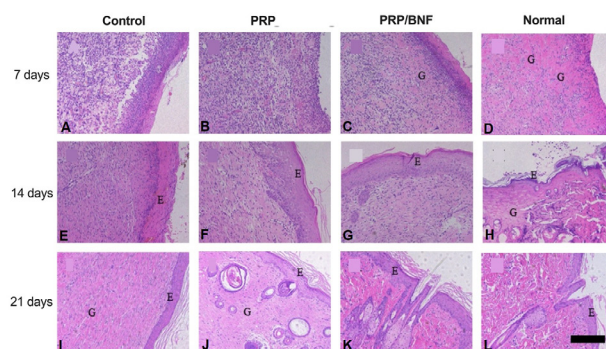


Fig. 5. Histopathological changes of deep second-degree scald treated with PRP/BNF by H & E staining (A to L, E=epidermis, G=granulation tissue, ×400); Histopathological score of PRP/BNF for deep second-degree scald wound in rats (n=5, \*P<0.05).

*Histopathological scoring and repair of wound tissue*

Figure 5 depicts a pathological slice of normal skin tissue. Scald wounds of both groups showed some epithelial cell proliferation, inflammation, edema and dispersion of collagen follicles on the 3<sup>rd</sup> day after scalding; nonetheless,

hair follicles were still present (Fig. 5). In the PRP/BNF group, capillaries were also seen (Fig. 5).

Both groups saw necrotic tissue fall off the skin 14 days after scalding, but the epithelial cells on the wound edge grew considerably and strengthened the skin. In the PRP/BNF group, epidermal hyperplasia was clearly seen surrounding the incision, and the mastoid layer was clearly visible (Fig. 5). The formation of granulation tissue, fibroblasts and new blood vessels, and inflammatory cells were observed in the dermis of each group. To put it another way, the dermis of those who took part in the study had a higher concentration of collagen than those in the control group (Fig. 5).

Epidermis continued to thicken and re-epithelialization was not complete on the 21<sup>st</sup> day following the burn. The new epithelium was surrounded by a layer of granulation tissue. The dermis was found to have fibrous hyperplasia and a disorganized structure. There were no visible skin appendages, despite the apparent invasion of inflammatory cells. Although the new epidermis formed in the PRP group showed the creation of a papillary layer, the various layers of this newly formed epidermis were not well distinguished. This group of patients had a skin tissue structure that was nearly complete; epidermis and dermal layers had been clearly divided, the new epithelial structure had become thinner and closer to normal skin's thickness, and new collagen fibers had been placed in the dermis layer. Hair follicles and sweat glands proliferated due to the presence of inflamed cells (Fig. 5).

At 3, 7, 14, and 21 days after scalding, the histopathological scores of each group are displayed in Figure 5. The histological scores of the PRP/BNF and PRP groups were higher than the control group's on days 7, 14, and 21 ( $P<0.05$ ), and the histopathological scores of the PRP/BNF group were higher than the PRP group's on day 21 ( $P<0.05$ ).

#### Effect of PRP/BNF on expression of injury related genes

Figure 6A, C, and D exhibit *IL-1*, *IL-6*, and *IL-10* mRNA expression. *IL-1*, *IL-6*, and *IL-10* mRNA expression rose in each group 3 days after damage, but there was no significant difference after scald. On day 7, *IL-1* and *IL-10* mRNA expression increased in the control and PRP groups, but PRP/BNF levels dropped ( $P<0.05$ ). *IL-6* mRNA expression reduced in each group 7 days after scald, although not significantly. On the 14<sup>th</sup> day, after modeling, *IL-6* and *IL-10* mRNA expression in each group was significantly lower than before, and *IL-6* and *IL-10* mRNA expression in the PRP/BNF group and PRP group was lower than that in the control group. KGF mRNA expression rose after burns and recovered to normal on day 21. No statistical change after scalding (Fig. 6B).

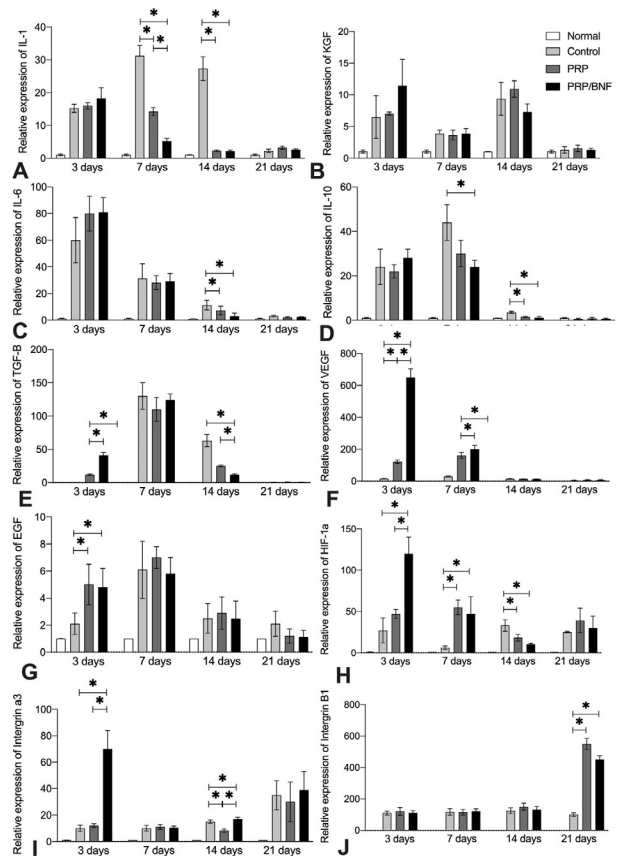


Fig. 6. Results of qPCR of wound-related genes at different time points on the surface of deep second-degree scalded wounds treated with PRP/BNF in rats ( $n=5$ ,  $*P<0.05$ ).

Figure 6E depicts *TGF-β* mRNA expression. 3 days after injury, each group's *TGF-β* mRNA increased. PRP/BNF was greater than PRP ( $P<0.05$ ), and PRP/BNF was higher than PRP group. The rise peaked on day 7 but wasn't statistically significant. After modeling, *TGF-β* mRNA expression reduced in all groups on day 14, although PRP/BNF dropped less than PRP and control ( $P<0.05$ ). On day 21, *TGF-β* mRNA reduced in wound tissues in both groups.

Figure 6F shows each group's *VEGF* mRNA expression 3 days after damage. *VEGF* mRNA was greater in glue than debridement glue ( $P<0.05$ ). Each group had elevated *VEGF* mRNA on day 7. PRP/BNF and PRP expressed more than control ( $P<0.05$ ). On day 14, *VEGF* mRNA expression increased and remained high in both groups ( $P>0.05$ ). On day 21, *VEGF* mRNA expression reduced in both groups ( $P>0.05$ ).

On day 3 following injury, PRP and PRP/BNF showed greater *EGF* mRNA expression than the control group (Fig. 6G) ( $P<0.05$ ). After modeling, *EGF* mRNA expression remained high in both groups on day 7

( $P>0.05$ ). *EGF* mRNA expression reduced on days 14 and 21, but not significantly ( $P>0.05$ ).

Figure 6H shows each group's *HIF-1* mRNA expression. On day 3 after injury, *HIF-1* mRNA expression was greater in PRP/BNF than PRP and control ( $P<0.05$ ). PRP/BNF and PRP had elevated *HIF-1* mRNA on day 7 ( $P<0.05$ ). PRP/BNF and PRP exhibited decreased *HIF-1* mRNA expression than control on day 14 ( $P<0.05$ ). 21 days after scorching, *HIF-1* mRNA expression didn't change ( $P>0.05$ ).

On day 3 following wound damage, *integrin 3* mRNA expression rose in all groups, but the PRP/BNF group showed a substantially larger rise than the control and PRP groups ( $P<0.05$ ), as shown in Figure 6I. ( $P<0.05$ ). Scald did not influence *integrin 3* mRNA expression on days 7 and 21 ( $P>0.05$ ).

Figure 6J displays *integrin1* mRNA levels. On days 3, 7, and 14, *integrin 1* mRNA expression rose in each group, although not significantly ( $P>0.05$ ). On day 21, PRP/BNF and PRP had increased *integrin 1* mRNA expression than the control group, although the difference between the two groups was not significant ( $P>0.05$ ).

## DISCUSSION

In the current study, we found that wound healing rates in the PRP/BNF group and PRP group were greater than those in the model group at each time point in the current investigation. *IL-1*, *IL-6*, and *IL-10* mRNA expression was considerably lower in the PRP/BNF group than in the untreated group, although *VEGF*, *EGF*, *TGF- $\beta$* , *HIF-1*, *integrin 1*, and *integrin 3* mRNA expression was significantly greater in both groups.

Sodium alginate PRP dressings also have proper properties. Biocompatibility, is widely used in wound dressings (Lemaître et al., 2011). As shown in this study, the scab removal time of the PRP/BNF group was much shorter than that of other groups, showing that PRP/BNF can speed up wound healing by encouraging necrotic tissue to be shed early, which is beneficial to wound healing. It appears that PRP/BNF has the ability to speed up the healing process of scald wounds since their wound healing rates were consistently greater than those of the model group at all time points. To compare histopathological scores from 7, 14, and 21 days after surgery, the PRP/BNF group had better results than the model group, whereas the PRP group had better results on day 21 than both the PRP/BNF and PRP groups together. It demonstrates that both the PRP/BNF and PRP may increase the quality of wound healing, but the PRP/BNF improves the quality of wound healing more than that of the PRP.

The first step in burn recovery is to reduce

inflammation. Early and moderate inflammation is important for wound repair, while excessive inflammation is not helpful to wound healing. PRP and PRP/BNF reduced *IL-6* and *IL-1* mRNA expression on the 14<sup>th</sup> day, but the expression of *IL-10* mRNA did not increase, indicating that PRP and PRP/BNF inhibit scald inflammation by decreasing IL-6 and IL-1 release, rather than increasing the expression of anti-inflammatory factors, as previously reported. Both the PRP/BNF and PRP have been shown to minimize the infiltration of inflammatory cells, which further supports the idea that the PRP/BNF and the PRP can enhance wound healing by lowering inflammation. The healing of wounds is inseparable from the important role of granulation tissue. Capillaries are the main component of granulation tissue, which can provide rich nutrients to the wound and improve the circulatory metabolism of the wound. VEGF is the main regulator of angiogenesis. It can activate endothelial cells and induce the formation of new blood vessels. It is the strongest growth factor in the growth factor family to promote the proliferation of endothelial cells. It is a key factor in determining wound angiogenesis (Ito et al., 2005). Studies have shown that epidermal stem cells (ESCs) can stimulate the proliferation of vascular endothelial cells by secreting VEGF and promote the formation of new blood vessels in the granulation tissue, which is beneficial to wound healing (Blanpain et al., 2006). From the results of this experiment, it was found that the expression of *VEGF* mRNA in the PRP/BNF group was higher than that in the model group, and pathologically, the early neovascularization of the PRP/BNF group was also higher than that in the model group, indicating that the PRP/BNF can promote wound regeneration in the early stage. The formation of blood vessels is beneficial to early improvement of blood circulation at the burn repair site and promote wound healing. Its effect may also be related to the activation of cytoskeletal calmodulin by calcium ions in the PRP to increase the expression of *VEGF* (Heidari et al., 2016).

In the early stage of wound healing, fibroblasts can up-regulate the expression of TGF- $\beta$ . At the same time, TGF- $\beta$  can also stimulate the proliferation of fibroblasts and regulate the synthesis of the extracellular matrix. In the later stage of wound healing, fibroblasts can pass negative feedback and inhibit the excessive secretion of TGF- $\beta$  (Navsaria et al., 2004). From the results of this experiment, it can be seen that on the 3<sup>rd</sup> day after scald, the expression of TGF- $\beta$  mRNA in each group increased, and the PRP/BNF group was higher than the PRP group and the model group, and more TGF- $\beta$  could stimulate fibroblasts. The proliferation and synthesis of more collagen are conducive to wound healing; it showed a downward trend on the 14<sup>th</sup> day after scald, suggesting that the PRP/BNF can inhibit

the expression of TGF- $\beta$  in the late stage of wound repair, thereby reducing the deposition of collagen in the late stage of wound healing. The HE pathological results showed that there were more fibroblasts in the PRP/BNF group than in the model group till 14<sup>th</sup> day; It is suggested that the PRP/BNF may promote the deposition of collagen by promoting the proliferation of fibroblasts, which is helpful for wound healing. EGF is secreted by fibroblasts and is a mitogenic stimulator of cells. It acts on keratinocytes in the form of paracrine to accelerate cell division, promote cell proliferation and migration, and accelerate the process of wound re-epithelialization (Lu and Fuchs, 2014). The results of this experiment showed that the EGF mRNA content of the PRP/BNF group and the PRP group on the third day was significantly higher than that of the model group, suggesting that the PRP/BNF and PRP may increase the level of EGF, and then promote skin cell proliferation and wound surface Repair.

The keratinocyte growth factor (KGF) is very important in the re-epithelialization process of wounds. It can induce the migration and proliferation of keratinocytes (basal keratinocytes are ESCs), thereby promoting the re-epithelialization of wounds (Sun *et al.*, 2014). After skin damage, KGF mainly comes from fibroblasts (Chelly *et al.*, 1999). In this experiment, the wounds of each group after scald had fibroblast proliferation, so the secretion of KGF is also higher than that of the normal group, which is conducive to wound healing. Studies have shown that HIF-1 $\alpha$  can accelerate the re-epithelialization of wounds by promoting the migration of ESCs (Stroka *et al.*, 2001). In this experiment, the expression of HIF-1 $\alpha$  mRNA in the PRP/BNF group was higher than that in the model group in the early stage, indicating that the PRP/BNF can increase the expression of HIF-1 $\alpha$  in the wound and promote the re-epithelialization of the wound. A variety of growth factors (TGF- $\beta$ , EGF, etc.) induce the proliferation and differentiation of fibroblasts, and the hypoxic microenvironment can further enhance the expression and activity of fibroblasts (Petrova *et al.*, 2018), so the PRP/BNF can also improve the growth of various wounds. The expression of factors (TGF- $\beta$ , EGF, VEGF) shortens the time of wound healing, which is resulted in the re-epithelialization of the wound. Other studies have shown that integrin plays an important role in the migration of keratinocytes. The results of this experiment found that the level of *integrin  $\alpha$ 3* mRNA in the PRP/BNF group was higher than that in the model group, suggesting that the PRP/BNF may promote the expression of *integrin  $\alpha$ 3*, thereby promoting the ability of keratinocyte migration and promoting wound re-epithelialization.

By providing a moist, hypoxic microenvironment, enhancing blood circulation, and increasing local growth

factors such as EGF, TGF-, and VEGF, the PRP/BNF may promote the proliferation and differentiation of ESCs; this may speed up wound healing; it may also promote collagen deposition; and it may improve the quality of wound healing. Integrin 1 and 3 expression is also promoted by PRP/BNF, which helps to enhance the link between the neonatal epithelium and its basement membrane. In addition, the PRP/BNF has a greater potential to enhance sweat gland proliferation and hair follicle creation.

Re-epithelialization of the wound, shortening the healing period, and improving healing quality can be facilitated by the use of PRP/BNF and PRP. Additionally, the PRP is more effective in repairing skin appendages such as sweat glands. For deep second-degree scald wounds to heal, PRP/BNF plays an important role in providing a hypoxic and humid environment, encouraging collagen deposition, reducing inflammation, and encouraging the migration and proliferation of epithelial cells in the early stages of the scald. In the late stages of scald, the high expression of integrin 1, HIF-1, and integrin 3 is linked to the high expression mechanism of integrin 1.

## CONCLUSION

In this study we observed that the PRP/BNFs and PRP can decrease the wound healing time and enhance the healing quality primarily by boosting the expression of VEGF, TGF-, HIF-1, Integrin 3, and Integrin 1 and lowering the expression of IL-1, IL-6, and IL-10.

## ACKNOWLEDGMENT

This work was supported by the AJA University of Medical Sciences.

### *Ethical approval*

All applicable international, national, and/or institutional guidelines for the care and use of animals were followed under Research Ethics Committees approval ID: IR.AJAUMS.REC.1400.080.

### *Statement of conflict of interest*

The authors have declared no conflict of interest.

## REFERENCES

- Afsar, F.S., Ergin, M., Ozek, G., Vergin, C., Karakuzu, A., and Seremet, S., 2017. Late-onset self-healing langerhans cell histiocytosis: Report of a very rare entity. *Rev. Paul. Pediatr.*, **35**: 115-119. <https://doi.org/10.1590/1984-0462/2017;35;1;00015>
- Blainpain, C. and Fuchs, E., 2009. Epidermal



- homeostasis: A balancing act of stem cells in the skin. *Nat. Rev. Mol. Cell Biol.*, **10**: 207-217. <https://doi.org/10.1038/nrm2636>
- Blanpain, C., Lowry, W.E., Pasolli, H.A., and Fuchs, E., 2006. Canonical notch signaling functions as a commitment switch in the epidermal lineage. *Genes Dev.*, **20**: 3022-3035. <https://doi.org/10.1101/gad.1477606>
- Cao, P.F., Xu, Y.B., Tang, J.M., Yang, R.H. and X.S. Liu, 2014. Hoxa9 regulates angiogenesis in human hypertrophic scars: Induction of vegf secretion by epidermal stem cells. *Int. J. clin. exp. Pathol.*, **7**: 2998.
- Chelly, N., Mouhieddine-Gueddiche, O.B., Barlier-Mur, A.M., Chailley-Heu, B., and Bourbon, J.R., 1999. Keratinocyte growth factor enhances maturation of fetal rat lung type ii cells. *Am. J. Respir. Cell mol. Biol.*, **20**: 423-432. <https://doi.org/10.1165/ajrcmb.20.3.3201>
- Choi, H.R., Byun, S.Y., Kwon, S.H. and Park, K.C., 2015. Niche interactions in epidermal stem cells. *World J. Stem Cells*, **7**: 495. <https://doi.org/10.4252/wjsc.v7.i2.495>
- Eldad, A., Weinberg, A., Breiterman, S., Chaouat, M., Palanker, D., and Ben-Bassat, H., 1998. Early nonsurgical removal of chemically injured tissue enhances wound healing in partial thickness burns. *Burns*, **24**: 166-172. [https://doi.org/10.1016/S0305-4179\(97\)00086-7](https://doi.org/10.1016/S0305-4179(97)00086-7)
- Harrison, C., Gossiel, F., Bullock, A., Sun, T., Blumsohn, A. and Mac-Neil, S., 2006. Investigation of keratinocyte regulation of collagen I synthesis by dermal fibroblasts in a simple in vitro model. *Br. J. Dermatol.*, **154**: 401-410. <https://doi.org/10.1111/j.1365-2133.2005.07022.x>
- Heidari, F., Yari, A., Rasoolijazi, H., Soleimani, M., Dehpoor, A., Sajedi, N. and Nobakht, M., 2016. Bulge hair follicle stem cells accelerate cutaneous wound healing in rats. *Wounds Compend. Clin. Res. Pract.*, **28**: 132-141.
- Ito, M., Liu, Y., Yang, Z., Nguyen, J., Liang, F., Morris, R.J., and Cotsarelis, G., 2005. Stem cells in the hair follicle bulge contribute to wound repair but not to homeostasis of the epidermis. *Nat. Med.*, **11**: 1351-1354. <https://doi.org/10.1038/nm1328>
- Iwamoto, H., Sakai, H., Tada, S., Nakamuta, M., and Nawata, H., 1999. Induction of apoptosis in rat hepatic stellate cells by disruption of integrin-mediated cell adhesion. *J. Lab. clin. Med.*, **134**: 83-89. [https://doi.org/10.1016/S0022-2143\(99\)90057-4](https://doi.org/10.1016/S0022-2143(99)90057-4)
- Janes, S.M., Lowell, S. and Hutter, C., 2002. Epidermal stem cells. *J. Pathol. J. Pathol. Soc. Great Br. Ireland*, **197**: 479-491. <https://doi.org/10.1002/path.1156>
- Kenny, F.N. and Connelly, J.T., 2015. Integrin-mediated adhesion and mechano-sensing in cutaneous wound healing. *Cell Tissue Res.*, **360**: 571-582. <https://doi.org/10.1007/s00441-014-2064-9>
- Lemaître, G., Nissan, X., Baldeschi, C. and Peschanski, M., 2011. Concise review: Epidermal grafting: The case for pluripotent stem cells. *Stem Cells*, **29**: 895-899. <https://doi.org/10.1002/stem.636>
- Levy, V., Lindon, C., Zheng, Y., Harfe, B.D., and Morgan, B.A., 2007. Epidermal stem cells arise from the hair follicle after wounding. *FASEB J.*, **21**: 1358-1366. <https://doi.org/10.1096/fj.06-6926com>
- Lu, C. and Fuchs, E., 2014. Sweat gland progenitors in development, homeostasis, and wound repair. *Cold Spring Harb. Perspect. Med.*, **4**: a015222. <https://doi.org/10.1101/cshperspect.a015222>
- Morasso, M.I. and Tomic-Canic, M., 2005. Epidermal stem cells: The cradle of epidermal determination, differentiation and wound healing. *J. Cell Biol.*, **97**: 173-183. <https://doi.org/10.1042/BC20040098>
- Navsaria, H.A., Ojeh, N.O., Moiemmen, N., Griffiths, M.A. and Frame, J.D., 2004. Reepithelialization of a full-thickness burn from stem cells of hair follicles micrografted into a tissue-engineered dermal template (integra). *Plast. Reconstr. Surg.*, **113**: 978-981. <https://doi.org/10.1097/01.PRS.0000105632.86651.EF>
- Peacock, H.M., Gilbert, E.A. and Vickaryous, M.K., 2015. Scar-free cutaneous wound healing in the leopard gecko, *Eublepharis macularius*. *J. Anat.*, **227**: 596-610. <https://doi.org/10.1111/joa.12368>
- Petrova, V., Annicchiarico-Petruzzelli, M., Melino, G. and Amelio, I., 2018. The hypoxic tumour microenvironment. *Oncogenesis*, **7**: 1-13. <https://doi.org/10.1038/s41389-017-0011-9>
- Raghavan, S., Bauer, C., Mundschau, G., Li, Q. and Fuchs, E., 2000. Conditional ablation of  $\beta 1$  integrin in skin severe defects in epidermal proliferation, basement membrane formation, and hair follicle invagination. *J. Cell Biol.*, **150**: 1149-1160.
- Rio, D.C., Ares, M., Hannon, G.J. and Nilsen, T.W., 2010. Purification of rna using trizol (tri reagent). *Cold Spring Harb. Protoc.*, **2010**: pdb. prot5439. <https://doi.org/10.1101/pdb.prot5439>
- Stroka, D.M., Burkhardt, T., Desbaillets, I., Wenger, R.H., Neil, D.A., Bauer, C., Gassmann, M. and Candinas, D., 2001. Hif-1 is expressed in normoxic tissue and displays an organ-specific regulation under systemic hypoxia. *FASEB J.*, **15**: 2445-2453

- <https://doi.org/10.1096/fj.01-0125com>.
- Sun, B.K., Siprashvili, Z., and Khavari, P.A., 2014. Advances in skin grafting and treatment of cutaneous wounds. *Science*, **346**: 941-945. <https://doi.org/10.1126/science.1253836>
- Sun, X., Fu, X., Han, W., Zhao, M. and Chalmers, L., 2013. Epidermal stem cells: An update on their potential in regenerative medicine. *Expert Opin. Biol. Ther.*, **13**: 901-910. <https://doi.org/10.1517/14712598.2013.776036>
- Takeo, M., Lee, W., and Ito, M., 2015. Wound healing and skin regeneration. *Cold Spring Harb. Perspect. Med.*, **5**: a023267. <https://doi.org/10.1101/cshperspect.a023267>
- Truong, A.B., Kretz, M., Ridky, T.W., Kimmel, R., and Khavari, P.A., 2006. P63 regulates proliferation and differentiation of developmentally mature keratinocytes. *Genes Dev.*, **20**: 3185-3197. <https://doi.org/10.1101/gad.1463206>
- Tumbar, T., Guasch, G., Greco, V., Blanpain, C., Lowry, W.E., Rendl, M., and Fuchs, E., 2004. Defining the epithelial stem cell niche in skin. *Science*, **303**: 359-363. <https://doi.org/10.1126/science.1092436>
- Zhu, Y., Yin, X., Li, J., and Zhang, L., 2019. Overexpression of microrna-204-5p alleviates renal ischemia-reperfusion injury in mice through blockage of fas/fasl pathway. *Exp. Cell Res.*, **381**: 208-214. <https://doi.org/10.1016/j.yexcr.2019.04.023>